Current Trends in Biotechnology and Pharmacy
Vol. 20(2) 2963-2977 April 2026, ISSN 0973-8916 (Print), 2230-7303 (Online)
DOI: 10.5530/ctbp.2026.2.20

In silico binding studies of NodD proteins of *Bradyrhizobium yuanmingense* and *Rhizobium tropici* with flavonoids

Pavan Kumar Pindi[1*], Sanjeev Kumar Kothur [1], Tanaji Vasavi Latha[1], Pulala Raghuveer Yadav[2], Hussain Basha Syed[3]

[1] Department of Microbiology, Palamuru University, Mahabubnagar-509 001, Telangana, India
[2] Department of Biotechnology, Indian Institute of Technology Hyderabad, Kandi, Sangareddy-502284, Telangana, India
[3] Innovative Informatica Technologies, Hyderabad, Telangana, India

***Corresponding author:** pavankumarpindi@gmail.com

Abstract

Prokaryotic bacteria, such as *Rhizobium* engage in endosymbiosis with legume plants' roots. In this mutualistic relationship, bacteria obtain carbon from the plant, while the plant benefits from nitrogen-fixation. The formation of root nodules in leguminous plants is induced by flavonoids exuded by the plant roots, acting as chemo-attractants for symbiotic rhizobia. The interaction between these flavonoids and NodD proteins is crucial for the induction of nodulation genes, influencing host range specificity. The initial signal exchanged during nodule development involves the interaction of legume root-exuded flavonoids with rhizobial NodD proteins, representing an early checkpoint in the establishment of symbiosis. In this current work, we focused on studying the molecular level interactions of flavonoids, common inducers of other rhizobial NodD protein with F1JZX9 protein (Nod D1) of *Bradyrhizobium yuanmingense* along with Q02876 protein (Nod D1) and P32008 protein (Nod D2) of *Rhizobium tropici* by *In-silico* studies. Docking studies, sequence alignment analysis, and molecular dynamics simulation studies were all applied in the *in-silico* investigations of molecular level interactions of flavonoids with common inducers of other rhizobial NodD protein of *Bradyrhizobium yuanmingense* and *Rhizobium tropici*. From our *In Silico* analysis, it was revealed that Flavonoids Myricetin and Daidzen have the highest potential to induce the nodulation process via binding to Nod D1 and Nod D2 proteins respectively. This molecular level understanding of how these flavonoids are selectively attracted towards NodD proteins can help in prioritizing the most binding efficient flavonoid towards attaining sustainable agriculture.

Keywords: NodD protein, *Bradhyrhizobium yuanmingense, Rhizobium tropici,* Flavonoids, Molecular modeling, Docking, MD simulations.

Introduction

The prokaryotic bacteria interact with legume plants root to develop endosymbiosis, where in the bacteria acquire carbon from the plant and in turn the plant gets nitrogen fixed. *Rhizobium, Bradyrhizobium, Azorhizobium, Mesorhizobium, Sinorhizobium and Allorhizobium* causes the root nodules in leguminous plants (1). Along with this, some tropical legumes can also enter symbiotic partnerships with certain species of *Methylobacterium, Burkholderia* and *Ralstoni* (2). Legume root-exudate flavonoids act as chemo-attractants for symbiotic rhizobia. These flavonoids induce the nodulation genes mediated by NodD proteins. Flavonoids interaction with NodD plays a significant role in induction of nodulation genes, is important for

host range specificity. All legumes cannot form symbiosis with a single rhizobial strain and vice versa (3, 4). Legume root-exudate flavonoids act as chemo-attractants for symbiotic rhizobia. During nodule development, the first symbiotic signal exchanged between legumes and rhizobia is flavonoids from the plant interacting with rhizobial NodD proteins, an early checkpoint of the symbiosis (5). The induction of the nodulation genes requires NodD protein, a sensor of plant flavonoids. Hence NodD have an important role in host specificity (6). LysR family, transcriptional regulators encode NodD proteins (7). F1JZX9, Q02876 and P32008 are Nod d gene products involved in regulation of expression of nod genes. Rhizobia have nodD genes, *R. leguminosarum bv*. *Trifolii*, has one nodD gene and some have two to five copies of NodDas in *B. japonicum*, strain NGR234, *R. tropici* and *R. meliloti*. Inspite of nodD genes in all rhizobia, the symbiotic characteristics vary from one species to another. The strain having NodD homologues could have diverse flavonoid preferences (8). In symbiosis, Nod d gene product in the presence of flavonoids regulates the expression of nod genes. Understanding the molecular interactions will help us to improve the nodulation and thus the nitrogen fixation in legumes and few non leguminous plants. This basic insight of rhizobial host molecular interactions can pave the way for sustainable agriculture.

The ability of *Bradhyrhizobium yuanmingense* and *Rhizobium tropici* in *Arachis hypogaeal* and *Vigna radiata* respectively, to nodulate and fix nitrogen (9, 10). The current work focused on studying the interaction of flavonoids, common inducers (11-19) of other rhizobial NodD protein with F1JZX9 protein (Nod D1) of *Bradyrhizobium yuanmingense* along with Q02876 protein (Nod D1) and P32008 protein (Nod D2) of *Rhizobium tropici.* We have employed *In-Silico* techniques towards understanding on how these flavonoids are selectively attracted towards NodD proteins can help in prioritizing the most binding efficient flavonoid, which in turn can provide insights into the molecular mechanisms underlying root nodulation and may have implications for improving nitrogen fixation in agricultural systems.

Materials and Methods

Molecular docking and visualization

To prepare for the docking, we begin by obtaining protein 3D structures in PDB format. Since our proteins of interest are not available in their crystallographic form in RCSB Protein Data Bank, we have retrieve structures of F1JZX9 protein (Nod D1) of *Bradyrhizobium yuanmingense*, along with Q02876 protein (Nod D1) and P32008 protein (Nod D2) of *Rhizobium tropici* from the Uniprot database (20). Subsequently, we used BioVia Discovery Studio Visualizer version 17.2 (21) molecular visualization tool to meticulously inspect and rectify any structural irregularities, ensuring accuracy by addressing missing atoms or residues. Next, we initiated MGLTools and PyMOL to add hydrogen atoms to the protein using PyMOL's "AddH" tool, a critical step for precise hydrogen placement necessary for accurate docking calculations. Following this, within MGLTools, we assigned Gasteiger charges to the protein atoms using the "Assign Charges" tool, a crucial prerequisite for computing electrostatic interactions during the docking process. Finally, using MGLTools' "Prepare Protein" tool to convert the protein structure into the Autodock-compatible PDBQT format, encompassing essential details such as atom types and charges, vital for successful docking simulations, as explained in detail elsewhere (22-24). Retrieved the 3D structure of the ligands from Pubchem database (25) in SDF, which were taken to Biovia Discovery studio for energy minimization and converted to PDB format. Once the ligand structure is secured in pdb format, using the "Prepare Ligand" tool within MGLTools, which facilitates the conversion of the ligand structure into the Autodock-compatible PDBQT format. This format ensures that the ligand possesses essential information, including atom types and charges, required for accurate Autodock docking calculations. Molecular

Current Trends in Biotechnology and Pharmacy
Vol. 20(2) 2963-2977 April 2026, ISSN 0973-8916 (Print), 2230-7303 (Online)
DOI: 10.5530/ctbp.2026.2.20

Docking was performed using AutoDock version 1.5.6 (26) to identify the compounds binding energy, predicted IC_{50} values along with binding pose revealing molecular level interactions in detail. It employs two steps grid generation and docking. Grid generation builds a compound wall directing the ligand to bind in a particular area of the protein. Grid dimensions used are as follows: X-axis = 126, Y-axis =126 and Z-axis =126 with the spacing of 0.375. Lamarckian Genetic Algorithm (LGA) was employed to perform the molecular docking. LGA creates 2500000 evolutions and generates 27000 docking poses and finally shows us the top 10 best outfitted ligands with the protein. Proteins and ligands were energy minimized using BioVia Discovery Studio Visualizer version 17.2 (21) which was also used to analyze interactions at the molecular level between docked protein-ligand complexes. Energy minimized proteins and ligands were imported into Autodock software using mgl tools interface and were converted in to pdbqt files before proceeding further for blind docking procedure using standard protocol, explained in detail elsewhere (27).

Molecular dynamic simulations

Molecular dynamic simulations were performed to validate the binding interactions of the best binders and analyze those interactions at the atomic level using the default protocol of Desmond v3.6 module as described in detail elsewhere (28-30). In brief, OPLS 2005 force field (31) parameters have been applied to simulation TIP3P water models (32) at neutral pH conditions. Periodic boundary conditions were used to determine the specific size and shape of the water box buffered at 10 Å of the simulation box. During the equilibration process, Van der Waals and short-range electrostatic interactions were treated with a cut off of 9 Å and long-range electrostatic interactions were computed using the Particle Mesh Ewald method (33). A Reversible reference system propagation algorithm (RESPA) integrator (34) was used with a time step of 2 fs, and long-range electrostatics were computed every 6 fs. One system for each of the three simulations containing approximately 23633 atoms for the F1JZX9-Eriodictyol complex; 47245 atoms for the P32008-Daidzen complex and 44400 atoms for the Q02876-Myricetin complex respectively were equilibrated using Desmond in the NPT ensemble at 300 K temperature and 1 bar using the Nose-Hoover chain relaxation thermostat method along with Martyna-Tobias-Klein relaxation Barostat method with isotropic coupling style at 1ps and 2ps timescale respectively. Before starting the analysis, we made sure that all the simulations were carried out at the same temperature, pressure and volume conditions throughout the simulated timescale (35). As part of the simulation quality analysis, it was revealed that the simulated systems' average total energy remained approximately -59500 kcal/mol for the F1JZX9-Eriodictyol complex, -111500 kcal/mol for Q02876-Myricetin complex and -118500 kcal/mol for P32008-Daidzen complex respectively.

Sequence alignment and analysis

Multiple sequence alignment of NodD sequences was done using ClustalW program (36), using default parameters.

Results and Discussion

Results

Molecular docking stands out as a very robust and reliable approach in predicting the correct binding pose of ligands, peptides, proteins, and even nanomaterials (37, 38). Nonetheless, it inherently lacks the capacity to account for dynamic binding effects (39). Combining molecular docking with molecular dynamics has established itself as a well-established protocol, yielding highly potent inhibitors through an integrated approach that encompasses both static and dynamic considerations (40-42). So in this study we have performed molecular docking followed by molecular dynamics simulations to reveal molecular level interactions between F1JZX9 (Nod D1) of *Bradyrhizobium yuanmingense* Q02876 (Nod

D1) and P32008 (Nod D2) of *Rhizobium tropici* with flavonoids. 7Hydroxycoumarin, Biochanin, Chrysin, Daidzein, Delphinidin, Eriodictyol, Flavone, Genistein, Hesperetin, Kaempferol, Luteolin, Malvidin, Myricetin, Naringenin, Petunidin and Quercetin are the selected flavonoids for the present investigation. The docking studies revealed that all the currently investigated flavonoids have the good binding capability with interaction energies ranging from -5.29 Kcal./mol to -8.76 Kcal./mol. All the docking results have been presented in Table 1. Among all the tested flavonoids, Eriodictyol, Myricetin and Daidzen were shown to be having the best binding ability with F1JZX9 (Nod D1), Q02876 (Nod D1) and P32008 (Nod D2) respectively.

Table 1: Docking results of selected flavonoids with F1JZX9 (Nod D1) of *Bradyrhizobium yuanmingense* and Q02876 (Nod D1) P32008 (Nod D2) of *Rhizobium tropici.*

S. No	Compound	F1JZX9		Q02876		P32008	
		Binding Energy	Predicted IC50 values	Binding Energy	Predicted IC50 values	Binding Energy	Predicted IC50 values
1	7Hydroxycoumarin	-5.62	75.44 µM	-6.74	11.51 µM	-5.75	61.26 µM
2	Biochanin	-5.92	45.91 µM	-6.88	9.05 µM	-7.09	6.34 µM
3	Chrysin	-6.70	12.19 µM	-6.91	8.56 µM	-6.75	11.31 µM
4	Daidzein	-5.84	52.48 µM	-5.96	42.69 µM	-8.76	376.38 nM
5	Delphinidin	-6.49	17.55 µM	-6.75	11.27 µM	-6.66	13.11 µM
6	Eriodictyol	-7.59	2.74 µM	-7.97	1.45 µM	-7.28	4.64 µM
7	Flavone	-6.44	18.96 µM	-7.75	2.08 µM	-7.03	7.07 µM
8	Genistein	-6.17	30.02 µM	-6.81	10.25 µM	-7.42	3.62 µM
9	Hesperetin	-6.75	11.26 µM	-6.27	25.16 µM	-7.21	5.15 µM
10	Kaempferol	-6.97	7.81 µM	-7.26	4.78 µM	-8.04	1.28 µM
11	Luteolin	-7.26	4.79 µM	-6.71	12.16 µM	-7.88	1.66 µM
12	Malvidin	-5.29	131.72 µM	-7.43	3.58 µM	-6.41	20.06 µM
13	Myricetin	-6.03	37.85 µM	-8.36	739.57 nM	-8.27	861.74 nM
14	Naringenin	-7.11	6.14 µM	-7.53	3.00 µM	-7.20	5.29 µM
15	Petunidin	-6.57	15.41 µM	-6.53	16.31 µM	-7.55	2.95 µM
16	Quercetin	-7.08	6.41 µM	-6.46	18.48 µM	-7.44	3.53 µM

Note: µM = Micromolar ; nM = Nanomolar. Bold values are the best binders in terms of binding energies and predicted IC50 values.

Molecular docking interactions analysis of F1JZX9-Eriodictyol; Q02876-Myricetin complex and P32008-Daidzen

Eriodictyol flavonoid exhibited binding energy of -7.59 Kcal/mol and a pIC_{50} value of 2.74 micromolar when docked with F1JZX9 (Nod D1) protein with a hydrogen bond with Asp12 residue as shown in figure 1a and Table 2. While Myricetin flavonoid exhibited binding energy of -8.36Kcal/mol and a pIC_{50} value of 739.57nanomolar when docked with Q02876 (Nod D1) protein with hydrogen bonds with Leu133; Lys199, Gly201 and Asn202 residues as shown in figure 1b and Table 2.

Daidzenflavonoid exhibited binding energy of -8.76Kcal/mol and a pIC_{50} value of

376.38 nano molar when docked with P32008 (Nod D2) protein with hydrogen bonds with Arg204 and Glu272 residues, as shown in figure 1c and Table 2.

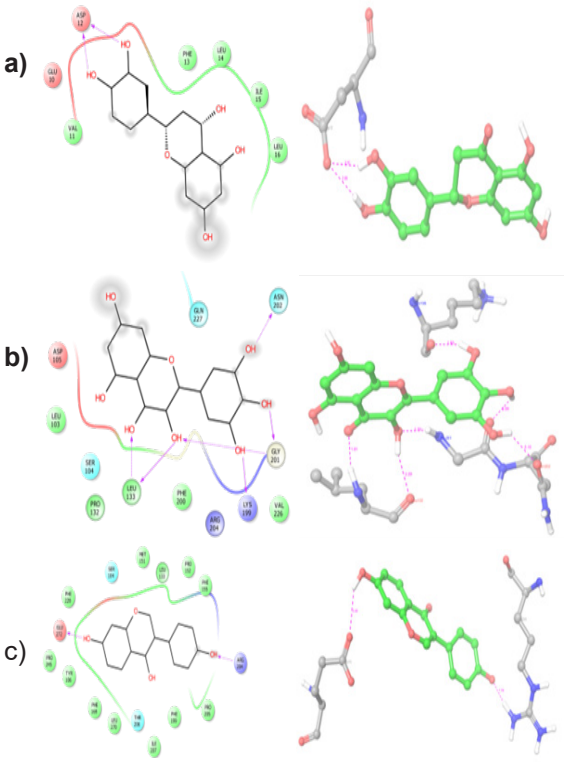

Figure 1: Molecular level interactions between a) F1JZX9-Eriodictyol complex b) Q02876-Myricetin complex and c) P32008-Daidzen complex. Left panel shows the interactions in 2D, whereas the right panel shows the interactions in three dimensional representations.

TMD simulations of F1JZX9-Eriodictyol; Q02876-Myricetin and P32008-Daidzen complexes

To understand the dynamics of the F1JZX9-Eriodictyol, Q02876-Myricetin and P32008-Daidzen complexes, we have performed three different molecular dynamic simulations of 100 nanoseconds (100000 picoseconds) each, i.e., a total of 300 nano seconds of simulation data has been collected for this study. In the first simulation, we simulated the F1JZX9-Eriodictyol complex. In the second simulation, we used the Q02876-Myricetin complex. And finally, in the third simulation, we have taken the P32008-Daidzen complex. To understand the impact of the flavonoid binding over the protein's structure dynamics, we have analyzed the Root mean square deviation (RMSD) of the protein backbone, energy parameter, and Secondary structural elements (SSE) percentage with reference to the simulated timescale. Protein's backbone RMSD was shown to be fluctuating between 2.0 and 6.0 Å, with an average of 5.0, 4.5 and 3.5Å for F1JZX9-Eriodictyol (figure 2a); Q02876-Myricetin (figure 2b) and P32008-Daidzen (figure 2c) complexes respectively. From the RMSD graph analysis (figure 2), it was evident that the P32008-Daidzen complex has shown much more stability in overall structure comparatively, while F1JZX9-Eriodictyol and Q02876-Myricetin complexes have demonstrated similar behavior as evident from RMSD graphs, especially after initial 40ns of simulated timescale.

Table 2: Hydrogen bonds exhibited by the selected flavonoids with F1JZX9 (Nod D1) of *Bradyrhizobium yuanmingense* and Q02876 (Nod D1) P32008 (Nod D2) of *Rhizobium tropici*:

S. No	Complex	No. of Hydrogen bonds	Amino acids involved in Hydrogen bonding
1.	F1JZX9-Eriodictyol	2	Asp12
2.	Q02876-Myricetin	6	Leu133; Lys199, Gly201 and Asn202
3.	P32008-Daidzen	2	Arg204 and Glu272

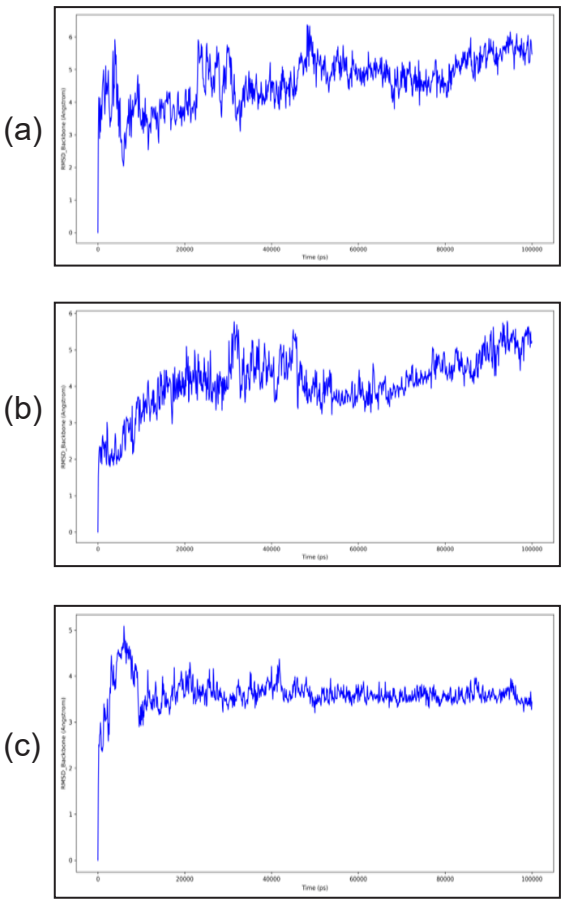

Figure 2: Root mean square deviation (RMSD) of protein backboneof a) F1JZX9-Eriodictyol complex b) Q02876-Myricetin complex and c) P32008-Daidzen complex. X-axis represents the timeline of the simulation in terms of picoseconds, whereas the y-axis represents the calculated RMSD in angstrom units.

To further confirm the role of flavonoids in stabilizing the complex of the P32008-Daidzen compared to F1JZX9-Eriodictyol and Q02876-Myricetin complexes, we have analyzed the RMSD of the molecules individually during the simulated timescale and observed that Daidzen molecule with an average of 0.6 Å RMSD is much more stable compared to Eriodictyol fluctuating interim upto 1.4 Å RMSD and Myricetin 1.0 Å RMSD as evident from the lower RMSD values (figure 3).

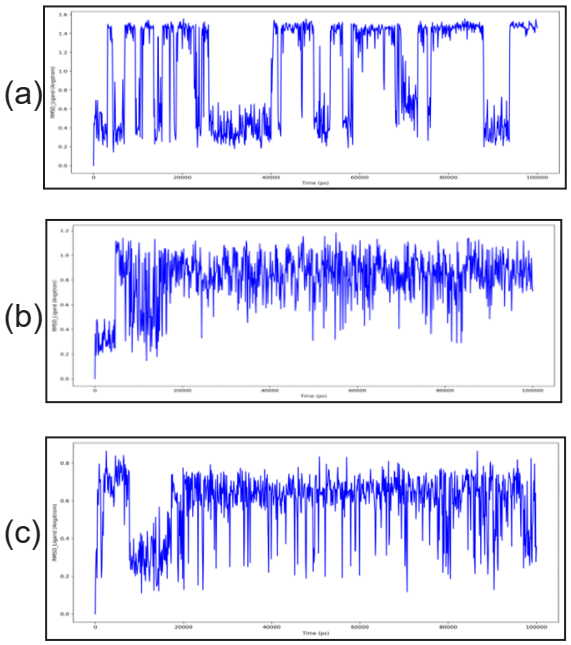

Figure 3: Root mean square deviation (RMSD) of flavonoids from the complexof a) F1JZX9-Eriodictyol complex b) Q02876-Myricetin complex and c) P32008-Daidzen complex. X-axis represents the timeline of the simulation in terms of picoseconds, whereas y-axis represents the calculated RMSD in angstrom units.

To further confirm the overall stability and inhibitory potential of the Eriodictyol, Daidzen and Myricetin flavonoids, we have analyzed the energy parameter of the simulated systems of F1JZX9-Eriodictyol, Q02876-Myricetin and P32008-Daidzen complexes.

The analysis it was revealed that potential energy of the simulated systems was approximately -74000, -138750 and -147500 Kcal/mol, for F1JZX9-Eriodictyol, Q02876-Myricetin and P32008-Daidzen complexes respectively. From this analysis, we can say that P32008-Daidzen (-147500 Kcal/mol) is being inhibited strongly, followed by Q02876-Myricetin (-138750 Kcal/mol) and F1JZX9-Eriodictyol (-74000 Kcal/mol) as evident with enormous negative binding energies (figure 4).

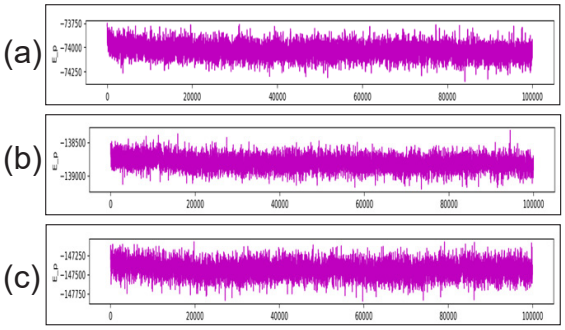

Figure 4: Calculated potential energies of the simulated systems of a) F1JZX9-Eriodictyol complex b) Q02876-Myricetin complex and c) P32008-Daidzen complex. X-axis represents the timeline of the simulation in terms of pico-seconds, whereas y-axis represents the calculated potential energy in kcal/mol units.

To further understand the impact of these flavonoids binding over the structural features of the proteins, we have investigated the secondary structural elements (SSE) of the F1JZX9 (Nod D1), Q02876 (Nod D1) and P32008 (Nod D2) proteins in the presence of Eriodictyol, Myricetin and Daidzen respectively with reference to the simulated timescale. As shown in Figure 5, the F1JZX9-Eriodictyol complex maintained an average of 38.89 % total SSE composed of 17.17% alpha helices and 21.72% beta helices and rest loops, Q02876-Myricetin complex maintained an average of 47.77 % total SSE composed of 30.56 % alpha helices and 17.21% beta helices and rest loops and P32008-Daidzen complex maintained an average of 46.71 % total SSE composed of 30.10 % alpha helices and 16.61% beta helices and rest loops.

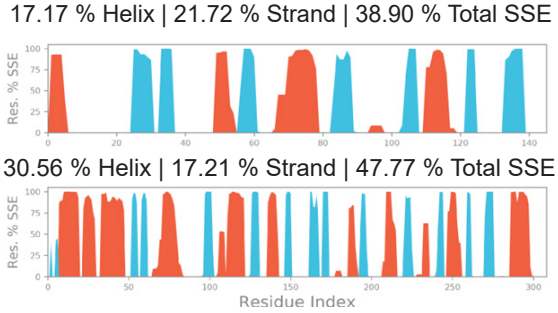

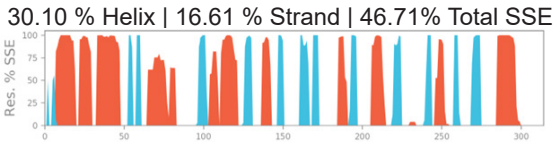

Figure 5: Analysis of Secondary Structural Elements (SSE) of a) F1JZX9-Eriodictyol complex b) Q02876-Myricetin complex and c). P32008-Daidzen complex. Protein secondary structure elements (SSE) like alpha-helices (orange colored) and beta-strands (blue colored) are monitored throughout the simulation. The plot above reports SSE distribution by residue index throughout the protein structure. X-axis represents the amino acid residues index, whereas the y-axis represents the calculated SSE percentage with reference to the simulated timescale.

Molecular interactions observed during molecular dynamic simulations

There were 34 contacts between the F1JZX9-Eriodictyol complexes, where 12 were involved in hydrogen bonds, 15 were involved in hydrophobic interactions and 23 were in water binding interactions. In the F1JZX9-Eriodictyol complex, the negatively charged interactions with Asp12, Ile15 and Glu138 along with pi-pi stacking with Trp142 were critically important in stabilizing (Figure 6).

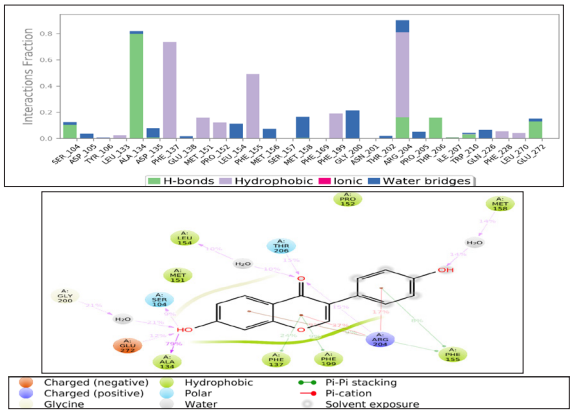

Figure 6: Molecular level interactions observed during the molecular dynamic simulations between F1JZX9-Eriodictyol complexes. Above bar chart panel is represented by the ligand interacting amino acid residues on x-axis and

interaction percentage with reference to simulated timescale on y-axis.

The Q02876-Myricetin complex found 23 contacts, out of which eight were involved in hydrogen bonds, five were involved in hydrophobic interactions and seventeen in water binding interactions respectively. Negatively charged interactions with Leu103, Leu133 and Gln227 were crucial in stabilizing the Q02876-Myricetin complex (Figure 7).

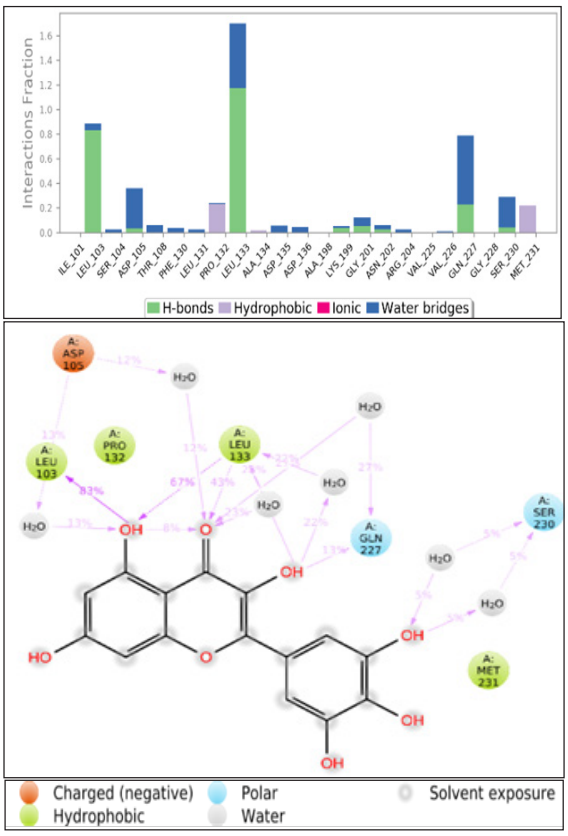

Figure 7: Molecular level interactions observed during the molecular dynamic simulations between Q02876-Myricetin complexes. Above bar chart panel is represented by the ligand interacting amino acid residues on x-axis and interaction percentage with reference to simulated timescale on y-axis.

Whereas, in the case of P32008-Daidzen complex, there found 29 contacts, out of which ten were engaged in hydrogen bonds, ten were involved in hydrophobic interactions and sixteen were in water binding interactions respectively. Negatively charged interactions with Thr206, Ser104, Glu272 and Ala134, along with pi-pi stacking with Phe137, Phe199, Arg204 and Phe155, were crucial in stabilizing the P32008-Daidzen complex (Figure 8).

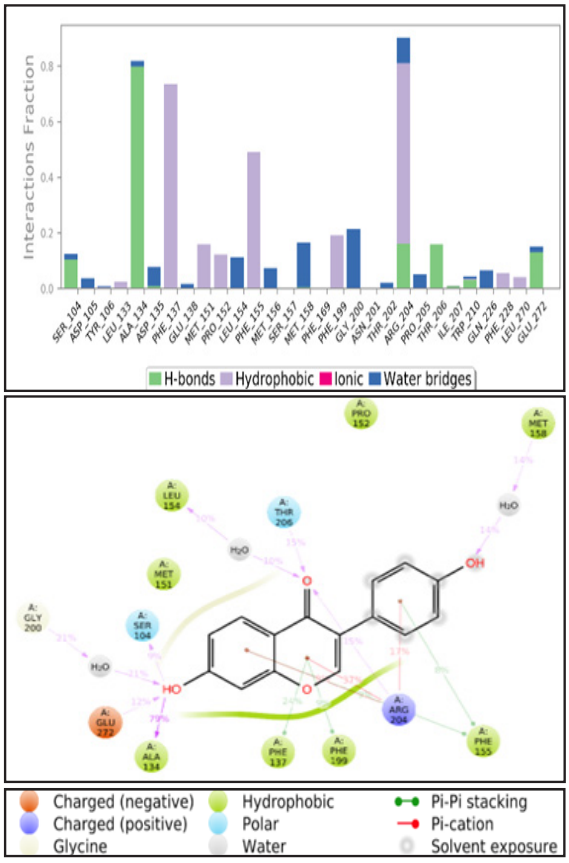

Figure 8: Molecular level interactions observed during the molecular dynamic simulations between P32008-Daidzen complexes. Above bar chart panel is represented by the ligand interacting amino acid residues on x-axis and interaction percentage with reference to simulated timescale on y-axis.

The results indicate that Non-Covalent interactions are responsible in the binding of flavonoid on the NodD Protein. NodD Proteins interacted differently with flavonoids based on their molecular weight, hydrophobicity, and ami-

Current Trends in Biotechnology and Pharmacy
Vol. 20(2) 2963-2977 April 2026, ISSN 0973-8916 (Print), 2230-7303 (Online)
DOI: 10.5530/ctbp.2026.2.20

no acid composition and sequence. The orientation of the B ring in the inducers, the presence of functional groups, their number and position linked to the backbone are the reason for the differences in the interaction with the NodD protein. The hydrogen bonding was seen between hydroxyl group of flavonoids and the oxygen or nitrogen of proteins. The hydrophobic interactions are due to the interactions between Non-polar aromatic ring of the flavonoids and hydrophobic regions of the protein molecules. The hydroxyl groups of flavonoids and charged groups on the proteins are responsible for electrostatic interactions.

Sequence and structural similarity analysis

To further understand the importance of structural difference contribution indifferent flavonoid preferences by NodD proteins. We have made a multiple sequence alignment between sequences of F1JZX9 protein (Nod D1) of *Bradyrhizobium yuanmingense* along with Q02876 protein (Nod D1) and P32008 protein (Nod D2) of *Rhizobium tropici.* As shown in figure 09, there is a striking divergence between the F1JZX9 protein (Nod D1) of *Bradyrhizobium yuanmingense* compared to the Q02876 protein (Nod D1) and P32008 protein (Nod D2) of *Rhizobium tropici.* The total number of amino acids in F1JZX9 protein encodedNod D1 of *Bradyrhizobium yuanmingense* was 148, whereas 308 and 314 for Q02876 protein (Nod D1) and P32008 protein (Nod D2) of *Rhizobium tropici.* This significant divergence was covered at the initial 135 amino acidswhile aligning the sequences. In three cases, NodD1 and NodD2 are most highly conserved at N-terminal halves and diverge towards C-terminal halves.

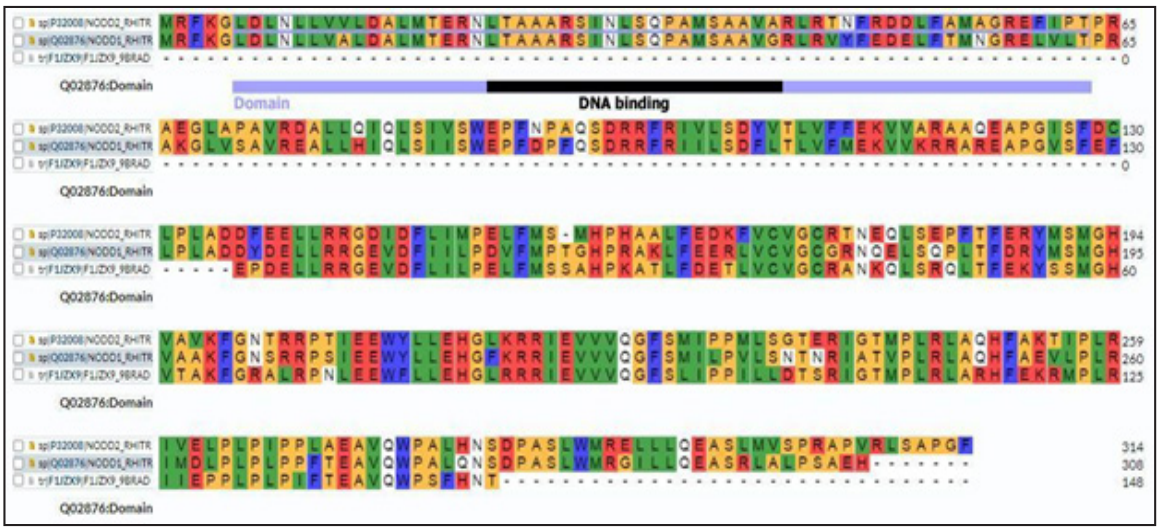

Figure 09: Sequence alignment between sequences of F1JZX9 protein (Nod D1) of *Bradyrhizobium yuanmingense* along with Q02876 protein (Nod D1) and P32008 protein (Nod D2) of *Rhizobium tropici.* DNA binding site is highlighted in black underline within protein domain highlighted in light blue.

The Uniprot database revealed that amino acids 6-63 contribute to the protein domain consisting of DNA binding site at amino acids 23-42 for both Q02876 protein (Nod D1) and P32008 protein (Nod D2) of *Rhizobium tropici.* From the analysis, it revealed that there are several amino acid differences between the proteins, as highlighted in white color in figure 10. V12A, A42G, T46V, N47Y, R49E, D50E, A53T, A55N, F59L, I60V and P61L are assumed to be crucial since there are within the proximity of the protein domain consisting of DNA binding site.

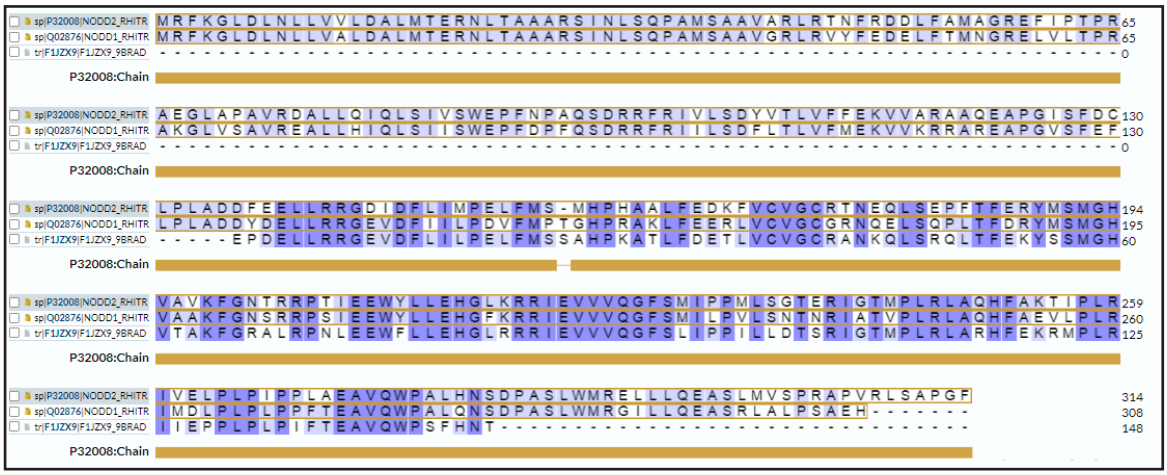

Figure 10: Sequence alignment between sequences of F1JZX9 protein (Nod D1) of *Bradyrhizobium yuanmingense* along with Q02876 protein (Nod D1) and P32008 protein (Nod D2) of *Rhizobium tropici.* Mutations were highlighted in white color.

Since there was significant difference betweentheF1JZX9 protein (Nod D1) of *Bradyrhizobium yuanmingense* compared to the Q02876 protein (Nod D1) and P32008 protein (Nod D2) of *Rhizobium tropici,* we have selected Q02876 protein (Nod D1) and P32008 protein (Nod D2) of *Rhizobium tropici* for further evaluation using structural superimposition. From the structural superimposition, as shown in figure 11, both Q02876 protein (Nod D1) and P32008 protein (Nod D2) of *Rhizobium tropici* have striking similarities, with the only difference being at the C-terminal due to the difference in number of amino acids.

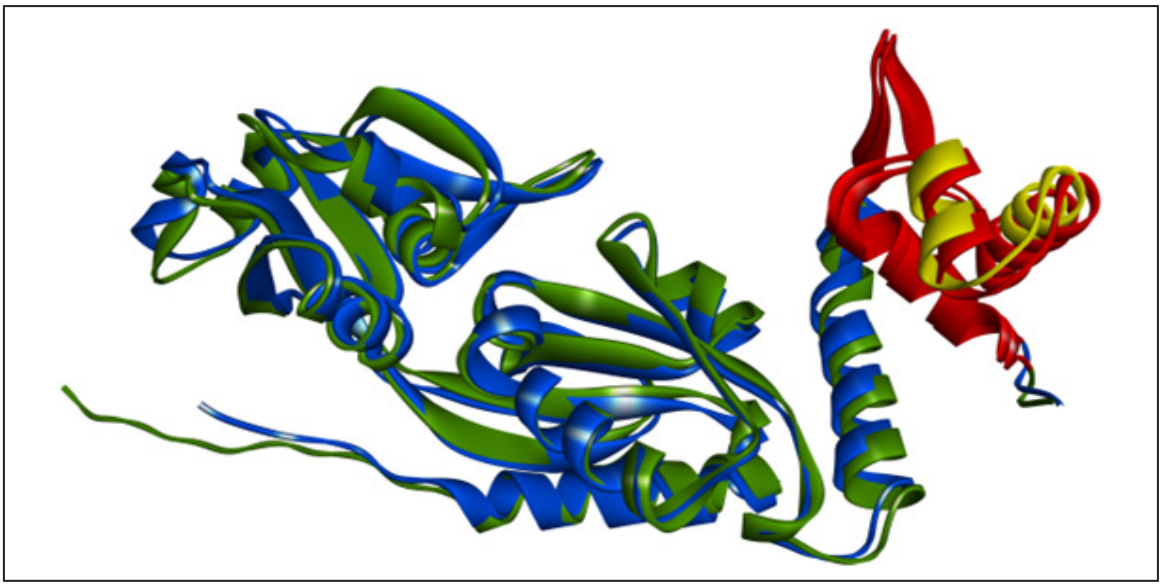

Figure 11: Superimposed structures of Q02876 (NodD1) P32008 (NodD2). Q02876 represented in Blue color, whereas P32008 is represented in Green color. Protein Domain was in Red color is highlighted with DNA binding helices in Yellow color.

Discussion

Sequence similarity analysis revealed several levels of divergence in terms of amino acids between the NodD genes, even from the same species and the difference noted in binding energies between selected flavonoids and nodD genes encoded proteins agreed with Wang et al., 2012 (3) remarks that no single rhizobial strains can form a symbiosis with all legumes, and vice versa. Specificity occurs at both species and genotypic levels (43-45). The docking and sequence alignment studies agreed with Györgypal *et al.*, 1991 (8) remarks that Legume root-exuded flavonoids act as chemo-attractants for symbiotic rhizobia. Our superimposition of the Q02876 protein (Nod D1) and P32008 protein (Nod D2) of *Rhizobium tropici* study also made it clear that although nodD genes are present in all rhizobia, their symbiotic characteristic may vary from one species to another, even in case of highly conserved protein structure similarities. A wide range of binding energy differences observed between -5.29 Kcal./mol to -8.76 Kcal./mol signifies that NodD homologues may have different flavonoid preferences even from the same strain. On the other hand, validation of docking studies with molecular dynamic simulations reveals that the highly conserved N-terminal amino acids play a critically important role in recognizing the flavonoids selectively. Further evaluation of Amino acids Glu138 from F1JZX9-Eriodictyol complex, Ala134 from P32008-Daidzen complex and Leu133 from Q02876-Myricetin complex is required as they were noteworthy. The molecular interaction findings (46, 47) between flavonoids and NodD proteins can help in understanding the biological nitrogen fixation. These insights can help to reduce the extensive use of nitrogen fertilizers and prevent their excessive use causing reduced biodiversity, eutrophication, and increasing antibiotic resistance.

Conclusion

In this study, we conducted *in-silico* investigations into the molecular interactions between selected flavonoids and NodD proteins involved in the root nodulation process of prokaryotic bacteria, specifically *Bradyrhizobium yuanmingense* (F1JZX9) and *Rhizobium tropici* (Q02876 and P32008). Our comprehensive analysis, combining docking studies and molecular dynamics simulations, provided valuable insights into the binding preferences, structural features, and dynamic behaviors of these interactions. The docking studies unveiled Eriodictyol, Myricetin, and Daidzen as the flavonoids with the highest binding abilities to F1JZX9 (Nod D1), Q02876 (Nod D1), and P32008 (Nod D2), respectively. Molecular dynamics simulations further elucidated the stability and potential energy landscapes of these flavonoid-protein complexes. Notably, the observed fluctuations in root mean square deviation (RMSD) and the substantial negative potential energy values underscored the robustness of these interactions. Our sequence alignment analysis of NodD proteins revealed amino acid variations, particularly at key positions (V12A, A42G, T46V, N47Y, R49E, D50E, A53T, A55N, F59L, I60V, and P61L), emphasizing their significance in the selective interaction with flavonoids. The highly conserved nature of the N-terminal amino acids, such as Glu138 in the F1JZX9-Eriodictyol complex, Ala134 in the P32008-Daidzen complex, and Leu133 in the Q02876-Myricetin complex, emerged as crucial elements in recognizing flavonoids selectively. Our findings align with previous research, reinforcing the concept that legume root-exuded flavonoids serve as chemo-attractants for symbiotic rhizobia. The observed variations in binding energies between flavonoids and NodD proteins from the same strain, as well as among different rhizobial species, support the notion of specificity at both species and genotypic levels. This study contributes to our understanding of the molecular mechanisms underlying the symbiotic relationship between leguminous plants and nitrogen-fixing bacteria. The identified flavonoids, Myricetin and Daidzen, emerge as promising inducers of the nodulation process, holding potential for applications in sustainable agriculture.

The identification of Myricetin and Daidzen as flavonoids with high binding potential to NodD proteins opens avenues for the design and synthesis of novel analogues. Designing structurally modified flavonoid analogues holds the promise of enhancing their specificity, affinity, and overall efficacy in inducing the nodulation process. Such tailored analogues could potentially exhibit improved binding characteristics, ensuring a more precise and efficient interaction with NodD proteins, thereby optimizing the symbiotic relationship between leguminous plants and rhizobia. Furthermore, the synthesis of novel flavonoid analogues provides an opportunity to address challenges such as bioavailability, stability, and potential off-target effects. Tailoring flavonoids for improved pharmacokinetic properties could enhance their practical applicability in agricultural settings. Additionally, the development of flavonoid analogues could contribute to the creation of environmentally friendly agrochemicals, reducing the dependence on conventional nitrogen fertilizers and mitigating associated ecological concerns. By deciphering the intricacies of flavonoid-NodD protein interactions, this research provides a foundation for targeted strategies aimed at enhancing biological nitrogen fixation, reducing reliance on nitrogen fertilizers, and mitigating the environmental impacts associated with their overuse. Further investigations into the highlighted amino acid residues and their roles in the symbiotic process will deepen our understanding of this crucial biological phenomenon.

Acknowledgements

The authors wish to acknowledge Department of Microbiology for their laboratory support. The authors are grateful to Prof. G N Srinivas, Vice-Chancellor, Palamuru University, Mahabubnagar for his encouragement and support.

Funding Source

No funding was received.

References

1. Gage, D.J., 2004. Infection and invasion of roots by symbiotic, nitrogen-fixing rhizobia during nodulation of temperate legumes. *Microbiology and molecular biology reviews*, *68*(2), pp.280-300.
2. Chen, W.M., Moulin, L., Bontemps, C., Vandamme, P., Béna, G. and Boivin-Masson, C., 2003. Legume symbiotic nitrogen fixation byβ-Proteobacteria is widespread inNature. *Journal of bacteriology*, *185*(24), pp.7266-7272.
3. Wang, D., Yang, S., Tang, F. and Zhu, H., 2012. Symbiosis specificity in the legume–rhizobial mutualism. *Cellular microbiology*, *14*(3), pp.334-342..
4. Liu, C.W. and Murray, J.D., 2016. The role of flavonoids in nodulation host-range specificity: an update. *Plants*, *5*(3), p.33..
5. Peck, M.C., Fisher, R.F. and Long, S.R., 2006. Diverse flavonoids stimulate NodD1 binding to nod gene promoters in Sinorhizobium meliloti. *Journal of bacteriology*, *188*(15), pp.5417-5427.
6. Spaink, H.P., Wijffelman, C.A., Pees, E., Okker, R.J. and Lugtenberg, B.J.J., 1987. Rhizobium nodulation gene nodD as a determinant of host specificity. *Nature*, *328*(6128), pp.337-340.
7. Long, S.R., 1996. Rhizobium symbiosis: Nod factors in perspective. *The Plant Cell*, *8*(10), p.1885.
8. Györgypal, Z., Kondorosi, E. and Kondorosi, A., 1991. Diverse signal sensitivity of NodD protein homologs from narrow and broad host range rhizobia..
9. Osei, O., Abaidoo, R.C., Ahiabor, B.D., Boddey, R.M. and Rouws, L.F., 2018. Bacteria related to Bradyrhizobium yuanmingense from Ghana are effective groundnut micro-symbionts. *Applied Soil Ecology*, *127*, pp.41-50.

10. Kumar, S. and Pindi, P.K., 2022. Host Specificity and Symbiotic Association Between InDigenous Rhizobium Strain and Arachis hypog. *Current Trends in Biotechnology and Pharmacy*, *16*(4), pp.456-470.

11. Recourt, K., Schripsema, J., Kijne, J.W., van Brussel, A.A. and Lugtenberg, B.J., 1991. Inoculation of Vicia sativa subsp. nigra roots with Rhizobium leguminosarum biovar viciae results in release of nod gene activating flavanones and chalcones. *Plant molecular biology*, *16*(5), pp.841-852.

12. Dakora, F.D., Joseph, C.M. and Phillips, D.A., 1993. Alfalfa (Medicago sativa L.) root exudates contain isoflavonoids in the presence of Rhizobium meliloti. *Plant Physiology*, *101*(3), pp.819-824.

13. Dakora, F.D., Joseph, C.M. and Phillips, D.A., 1993. Common bean root exudates contain elevated levels of daidzein and coumestrol in response to Rhizobium inoculation. *Molecular plant-microbe interactions*, *6*(5), pp.665-668.

14. Göttfert, M., 1993. Regulation and function of rhizobial nodulation genes. *FEMS microbiology reviews*, *10*(1-2), pp.39-63.

15. Schmidt, P.E., Broughton, W.J. and Werner, D., 1994. Nod factors of Bradyrhizobium japonicum and Rhizobium sp. NGR234 induce flavonoid accumulation in soybean root exudate.

16. Lawson, C.G., Rolfe, B.G. and Djordjevic, M.A., 1996. Rhizobium inoculation induces condition-dependent changes in the flavonoid composition of root exudates from Trifolium subterraneum. *Functional Plant Biology*, *23*(1), pp.93-101.

17. Bolaños-Vásquez, M.C. and Werner, D., 1997. Effects of Rhizobium tropici, R. etli, and R. leguminosarum bv. phaseoli on nod gene-inducing flavonoids in root exudates of Phaseolus vulgaris. *Molecular plant-microbe interactions*, *10*(3), pp.339-346.

18. Novák, K., Lisá, L. and Škrdleta, V., 2004. Rhizobial nod gene-inducing activity in pea nodulation mutants: dissociation of nodulation and flavonoid response. *Physiologia Plantarum*, *120*(4), pp.546-555.

19. Brechenmacher, L., Lei, Z., Libault, M., Findley, S., Sugawara, M., Sadowsky, M.J., Sumner, L.W. and Stacey, G., 2010. Soybean metabolites regulated in root hairs in response to the symbiotic bacterium Bradyrhizobium japonicum. *Plant Physiology*, *153*(4), pp.1808-1822.

20. Consortium, U., 2015. UniProt: a hub for protein information. *Nucleic Acids Res*, *43*(D1), pp.D204-D212. https://www.uniprot.org/

21. BIOVIA, D.S., 2017. BIOVIA discovery studio visualizer. *Software version*, *20*, p.779. https://discover.3ds.com/discovery-studio-visualizer-download

22. Pande, M., Kundu, D. and Srivastava, R., 2022. Vitamin C and Vitamin D3 show strong binding with the amyloidogenic region of G555F mutant of Fibrinogen A alpha-chain associated with renal amyloidosis: proposed possible therapeutic intervention. *Molecular Diversity*, *26*(2), pp.939-949.

23. Pande, M., Kundu, D. and Srivastava, R., 2023. Selective vitamins as potential options for dietary therapeutic interventions: in silico and in vitro insights from mutant C terminal fragment of FGA. *The Journal of Steroid Biochemistry and Molecular Biology*, *230*, p.106290.

24. Gupta, S. and Dasmahapatra, A.K., 2023. Enhanced stability of a disaggregated Aβ fibril on removal of ligand inhibits refibrillation: An all atom Molecular Dynamics simulation study. *International Journal of Biological Macromolecules*, *240*, p.124481.

25. Kim, S., Thiessen, P.A., Bolton, E.E., Chen, J., Fu, G., Gindulyte, A., Han, L., He, J., He,

S., Shoemaker, B.A. and Wang, J., 2016. PubChem substance and compound databases. *Nucleic acids research*, *44*(D1), pp.D1202-D1213.

26. Goodsell, D.S., Morris, G.M. and Olson, A.J., 1996. Automated docking of flexible ligands: applications of AutoDock. *Journal of molecular recognition*, *9*(1), pp.1-5.

27. Reddy, S.V.G., Reddy, K.T., Kumari, V.V. and Basha, S.H., 2015. Molecular docking and dynamic simulation studies evidenced plausible immunotherapeutic anticancer property by Withaferin A targeting indoleamine 2, 3-dioxygenase. *Journal of Biomolecular Structure and Dynamics*, *33*(12), pp.2695-2709.

28. Basha, S.H., Svs, S.P., Madar, I.H., Kousar, S.H., Jayanna, N. and Sultan, G., 2020. In-silico screening of Indian medicinal plants active constituents database revealed Gmelanone and Litseferine as potential 3CLpro antagonists targeting SARS-CoV-2. *J. PeerScientist*, *4*, p.e1000030..

29. Basha, S.H., Thakur, A. and Samad, F.A., 2016. Insights from the predicted structural analysis of carborane substituted withaferin A with Indoleamine-2, 3-dioxygenase as a potent inhibitor. *Bioinformation*, *12*(9), p.374.

30. Hassan, S.S.U., Zhang, W.D., Jin, H.Z., Basha, S.H. and Priya, S.S., 2022. In-silico anti-inflammatory potential of guaiane dimers from Xylopia vielana targeting COX-2. *Journal of Biomolecular Structure and Dynamics*, *40*(1), pp.484-498.

31. Shivakumar, D., Harder, E., Damm, W., Friesner, R.A. and Sherman, W., 2012. Improving the prediction of absolute solvation free energies using the next generation OPLS force field. *Journal of chemical theory and computation*, *8*(8), pp.2553-2558.

32. Mark, P. and Nilsson, L., 2001. Structure and dynamics of the TIP3P, SPC, and SPC/E water models at 298 K. *The Journal of Physical Chemistry A*, *105*(43), pp.9954-9960.

33. Essmann, U., Perera, L., Berkowitz, M.L., Darden, T., Lee, H. and Pedersen, L.G., 1995. A smooth particle mesh Ewald method. *The Journal of chemical physics*, *103*(19), pp.8577-8593.

34. Figueirido, F., Levy, R.M., Zhou, R. and Berne, B.J., 1997. Large scale simulation of macromolecules in solution: Combining the periodic fast multipole method with multiple time step integrators. *The Journal of chemical physics*, *106*(23), pp.9835-9849.

35. Shaikh, F., Bhakat, S., Thakur, A., Radadia, A., ES Soliman, M. and Shah, A., 2015. Identification of novel GSK1070916 analogs as potential aurora b inhibitors: insights from molecular dynamics and MM/GBSA based rescoring. *Letters in Drug Design & Discovery*, *12*(1), pp.2-13.

36. Thompson, J.D., Gibson, T.J. and Higgins, D.G., 2003. Multiple sequence alignment using ClustalW and ClustalX. *Current protocols in bioinformatics*, (1), pp.2-3.

37. Madhyastha, H., Madhyastha, R., Thakur, A., Kentaro, S., Dev, A., Singh, S., Kumar, H., Acevedo, O., Nakajima, Y., Daima, H.K. and Aradhya, A., 2020. c-Phycocyanin primed silver nano conjugates: Studies on red blood cell stress resilience mechanism. *Colloids and Surfaces B: Biointerfaces*, *194*, p.111211.

38. Badavath, V.N., Thakur, A., Shilkar, D., Nath, C., Acevedo, O., Ucar, G. and Jayaprakash, V., 2022. Brain permeable curcumin-based pyrazoline analogs: MAO inhibitory and antioxidant activity. *Journal of Molecular Structure*, *1268*, p.133681.

39. Meng, X.Y., Zhang, H.X., Mezei, M. and Cui, M., 2011. Molecular docking: a pow-

erful approach for structure-based drug discovery. *Current computer-aided drug design*, *7*(2), pp.146-157.

40. Gangadevi, S., Badavath, V.N., Thakur, A., Yin, N., De Jonghe, S., Acevedo, O., Jochmans, D., Leyssen, P., Wang, K., Neyts, J. and Yujie, T., 2021. Kobophenol A inhibits binding of host ACE2 receptor with spike RBD domain of SARS-CoV-2, a lead compound for blocking COVID-19. *The journal of physical chemistry letters*, *12*(7), pp.1793-1802.

41. Gangireddy, M.S.R., Badavath, V.N., Velez, C., Loeanurit, N., Thakur, A., Maddipati, V.C., Katari, N.K., Acevedo, O., Boonyasuppayakorn, S. and Gundla, R., 2022. Discovery of 3-chlorobenzyl-linked 1, 9-diazaspiro [5.5] undecane derivatives, a lead for dengue virus type 2 infection. *New journal of chemistry*, *46*(3), pp.1087-1098.

42. Siddique, M.U.M., Thakur, A., Shilkar, D., Yasmin, S., Halakova, D., Kovacikova, L., Prnova, M.S., Stefek, M., Acevedo, O., Dasararaju, G. and Devadasan, V., 2021. Non-carboxylic acid inhibitors of aldose reductase based on N-substituted thiazolidinedione derivatives. *European journal of medicinal chemistry*, *223*, p.113630.

43. Broughton, W.J., Jabbouri, S. and Perret, X., 2000. Keys to symbiotic harmony. *Journal of bacteriology*, *182*(20), pp.5641-5652.

44. Cooper, J.E., 2007. Early interactions between legumes and rhizobia: disclosing complexity in a molecular dialogue. *Journal of applied microbiology*, *103*(5), pp.1355-1365.

45. Perret, X., Staehelin, C. and Broughton, W.J., 2000. Molecular basis of symbiotic promiscuity. *Microbiology and Molecular Biology Reviews*, *64*(1), pp.180-201.

46. Dhankhar, P., Dalal, V., Singh, V., Tomar, S. and Kumar, P., 2022. Computational guided identification of novel potent inhibitors of N-terminal domain of nucleocapsid protein of severe acute respiratory syndrome coronavirus 2. *Journal of Biomolecular Structure and Dynamics*, *40*(9), pp.4084-4099.

47. Singh, V., Dhankhar, P., Dalal, V., Tomar, S., Golemi-Kotra, D. and Kumar, P., 2022. Drug-repurposing approach to combat Staphylococcus aureus: biomolecular and binding interaction study. *ACS omega*, *7*(43), pp.38448-38458.